J Mater Sci (2008) 43:4282–4289
DOI 10.1007/s10853-008-2622-1

Application of the electrochemical machining technique for the characterization of zinc coatings

S. M. A. Shibli · R. Manu

Received: 17 January 2006 / Accepted: 11 February 2008 / Published online: 23 April 2008

Abstract Electrochemical machining is a useful technique for characterizing the inner alloy structure of metallic coatings. In the present study, hot-dip zinc galvanized coatings were fabricated and the microstructures were analyzed after exposing each layer of the coatings by successive anodic machining steps. With this method, the surface after each successive machining step would be free from any mechanical damage or segregation of the dissolution products over the machined surface. The characteristics of the alloy layers and their influence on the behavior of the coatings were investigated under a specific exposure condition. The corrosion performance of the iron-rich inner alloy layers was found to be better than that of the pure zinc top layer as revealed during electrochemical characterization. This paper provides insight into the correlation between the protection strength of the galvanic coating and the quantity of zinc in the coating.

Introduction

There has been significant research activity involving the characterization of metallic coatings and their performance under various exposure conditions over the past decades [1, 2]. Of particular importance is the galvanization reaction for producing corrosion-resistant coatings on steels. The galvanization reactions form inter-metallic compounds in the Fe–Zn metal system. Considerable work has been performed to evaluate the thermodynamic properties of the system forming different inter-metallic compounds [3–8]. The coating weight can be estimated from the Fe content or the Fe equivalent and from the surface roughness of the steel substrate [9]. When these Zn-coated steel sheets are subjected to pressing operations, the adhesive wear, i.e. the wear due to localized bonding between the contacting solid surfaces leading to material transfer, can lead to degradation of the coating [10–12]. Detailed and deeper understanding of the microstructure and its impact on the coating tolerance are important in order to develop improved coatings. In this context, the exposure of the inner alloy layers and their microstructural and electrochemical characterization are significant from a corrosion protection point of view.

Electrochemical machining is a demonstrated and successful method for characterizing the inner alloy microstructure as well as the compositional variation in the coating layers compared to other conventional techniques [13, 14]. The high rate of metal dissolution (accelerated test) particularly under high current load and higher electrolyte flow rates are monitored to study the microscopic heterogeneities of the coating. Anodic machining is one of the advanced electrochemical processes for shaping the surface of metals by controlled anodic dissolution. Electrochemical machining is a unique application of controlled anodic dissolution as the surface of the machined metal is devoid of any mechanical damage. An advantage of the technique is the dimensional accuracy of the machined substrate. This technique is widely accepted for razor head projection, surface smoothing, and for various other systems [15, 16].

The present work utilizes the electrochemical machining technique for layer-wise characterization of hot-dip zinc coatings under one specific exposure condition. The objective of this study is to provide a correlation between

S. M. A. Shibli (✉) · R. Manu
Department of Chemistry, University of Kerala, Kariavattom Campus, Thiruvananthapuram, Kerala 695 581, India
e-mail: smashibli@yahoo.com

the protection performance of the galvanized coating and the quantity of zinc in the coating.

Experimental methods

The galvanizing process

The composition of the steel used in this investigation was: 0.09 C, 0.34 Mn, 0.036 P, 0.0487 Si, and 0.029 Al, balance Fe, all in wt%. Steel coupons, 5 cm × 5 cm × 0.1 cm in size, were used as the substrate and were given the standard pre-treatment prior to galvanization. Prior to galvanization, the steel coupons were pickled in 8% HCl solution, washed with distilled water, and then fluxed with 30% NH_4Cl solution. The temperature of the molten zinc bath was kept at 450±10 °C, and the immersion time was maintained at 15–20 s. The excess zinc over the surface of the coupons was removed by blowing hot air.

Electrochemical machining

In order to achieve the required extent of metal removal, the electrochemical dissolution process had to be controlled in terms of the current load, electrolyte flow rate, inter-electrode distance, and the exposed area. In the present case, a lower current density of about 10 mA/cm^2 was fixed, as the coating was several microns in thickness. At high current density, the coating would rapidly dissolve; hence, the potential change would not be precise at the high rate of metal removal. Normally, the nature of the electrolyte and its flow can influence the dissolution behavior and the surface glossiness of the galvanized coupons. A 3% NaCl solution was selected and used as the dissolution medium since it is non-passivating as well as more aggressive in terms of corrosive behavior compared to other electrolytes. The anode was the galvanized coupon, and a platinum mesh of larger surface area was used as the cathode for the electrochemical machining process. The inter-electrode gap was kept at 1 cm, and the electrolyte used was a 3% neutral (pH of 7) NaCl solution. The electrolyte was kept stagnant at 30 ± 2 °C.

Characterization of the machined coupons

The surface characterization of the anodically machined coating and the identification of the various phases were performed using atomic force microscopy (AFM) and scanning electron microscopy (SEM). The topographic analysis of the galvanized specimens was performed using a Molecular Imaging Pico Scan 2100 atomic force microscope in contact mode. A phosphate (n) doped silicon coated cantilever (force constant—0.05–3 N/m) was used for imaging. The height mode was used to scan the surface. The SEM characterization was performed using an Hitachi S 4000 SEM equipped with an Oxford Instruments energy dispersive X-ray spectrometer and analyzer. In addition, a GBC 932 Atomic Absorption Analyzer was used to determine the concentration profile of iron and zinc in the dissolution product formed during anodic dissolution machining of the coating. The analysis was performed at wavelengths of 213.9 nm for zinc and 248.3 nm wavelengths for iron. The flame was air-acetylene and the scan time was 3 s. From the absorbance of the standard solution the percentage of different elements in the sample were determined. The corrosion tolerance and the galvanic performance of the coating were also determined based on open circuit potential (OCP) decay measurements during long-term immersion tests.

Results and discussion

Surface morphology of the coating

The morphology of the galvanized coupons after each electrochemical machining step was evaluated using SEM (Fig. 1). The acceptability of galvanized coatings depends on the surface feature of the coating. The formation of very large grains, termed "spangles," which were visible on the zinc surface, depends on the galvanizing conditions. The outer pure Zn coating exhibited a structure consisting of typical coarse feather-like "spangles" over the entire coating. The outermost layer (η phase) is pure zinc, with a bright and smooth surface. The η phase is supposed to consist of Hexagonal Close Packing, with less than 0.05% iron content. With continued anodic machining, the morphology of the coating was characterized by the presence of an etched remnant phase that extended over the entire surface. The surface also contained regions of localized anodic dissolution. Figure 1c shows the surface morphology of the layer exposed after 8 h of anodic machining. The deeper regions had a smooth appearance and the slightly darker regions formed over the zinc layer are the zinc-depleted regions/inhomogeneous surface formed due to anodic machining Previous researchers had associated the presence of a ridged surface topography with the presence of coarse precipitates formed in Zn–Pb galvanized coatings [17–19]. Figure 1d and e shows the regions containing discrete micron-sized features. Continued anodic machining resulted in pronounced etched structures indicative of multiple phases. The presence of inner channels showed the absence of zinc after 10 h of anodic machining as evidenced during AAS analysis of the sample further dissolved. The inner alloy layers contained more iron-rich regions, as expected. The alloy layers were found

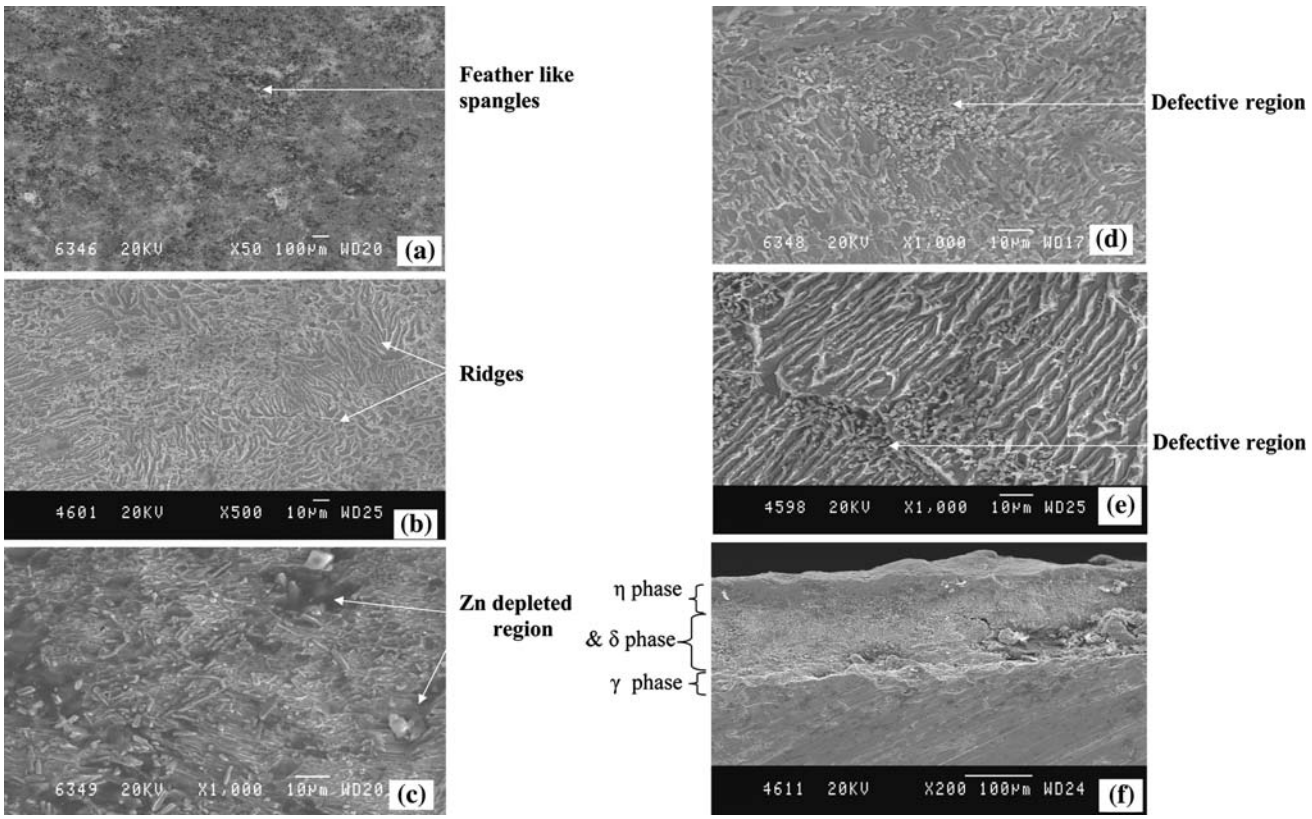

Fig. 1 SEM micrographs of the coatings after different periods of electrochemical machining (**a**): 4 h (**b**): 6 h (**c**): 8 h (**d**): 10 h (**e**): 12 h (**f**) Cross-sectional view of the zinc coating

to be generally porous in nature. The SEM image of the coating cross section is included in Fig. 1f. The different layers of the zinc coating formed on the steel during galvanization are identified in the figure.

AFM images of the pure zinc coating were recorded after two intervals of anodic machining (Fig. 2a and b). The 3D image revealed the topography of the coating. The average grain size of the zinc coating after 4 h of machining ($\sim$500 nm) was coarser than that of the grain size after 8 h of machining ($\sim$300 nm). As expected, after initial machining (Fig. 2a) the Zn grains exhibited an angular, facetted morphology, consistent with an as-solidified structure, whereas the grain morphology after 8 h of machining appeared globular. The height of the grains was uniform (Fig. 2b). The 3D image corresponding to the zinc coating after 4 h of anodic machining showed a coarse, rounded grain structure, as shown in Fig. 2a. The roughness value of the coating was also determined to assess the height variation of the coating. As expected, the outer surface exhibited the lowest roughness. As the extent of anodic machining increased, the roughness of the exposed surface increased, since these layers were more prone to undergo corrosion due to selective dissolution of the constituent phases. The zinc coating (Fig. 2b) consisted of globular shape and the grains could be clearly distinguished. The mean roughness values indicated that the initially exposed layers of the zinc coating had a roughness of $\sim$10 nm. The layers exposed after 8 h of electrochemical machining had roughness of $\sim$25 nm. The difference in the roughness value could be due to the variation in the microstructure within the coating.

The coating exposed after anodic machining was analyzed by XRD, as shown in Fig. 3, and was determined to consist of Fe and Zn. It is evident that as the extent of anodic machining process continues, a discrete secondary phase is formed as revealed by the iron content along with zinc in the inner alloy layers. EDX analysis (Fig. 4) confirmed that both Fe and Zn were present in the exposed layer of the coating.

Electrochemical characterization

In the present work, the different layers of the coating were exposed after successive anodic dissolution of the coating under an applied current. The OCP of the as-exposed surfaces after successive anodic dissolution steps was monitored with respect to a saturated calomel electrode. The zinc dissolved during the anodic machining process was determined after each interval by AAS analysis.

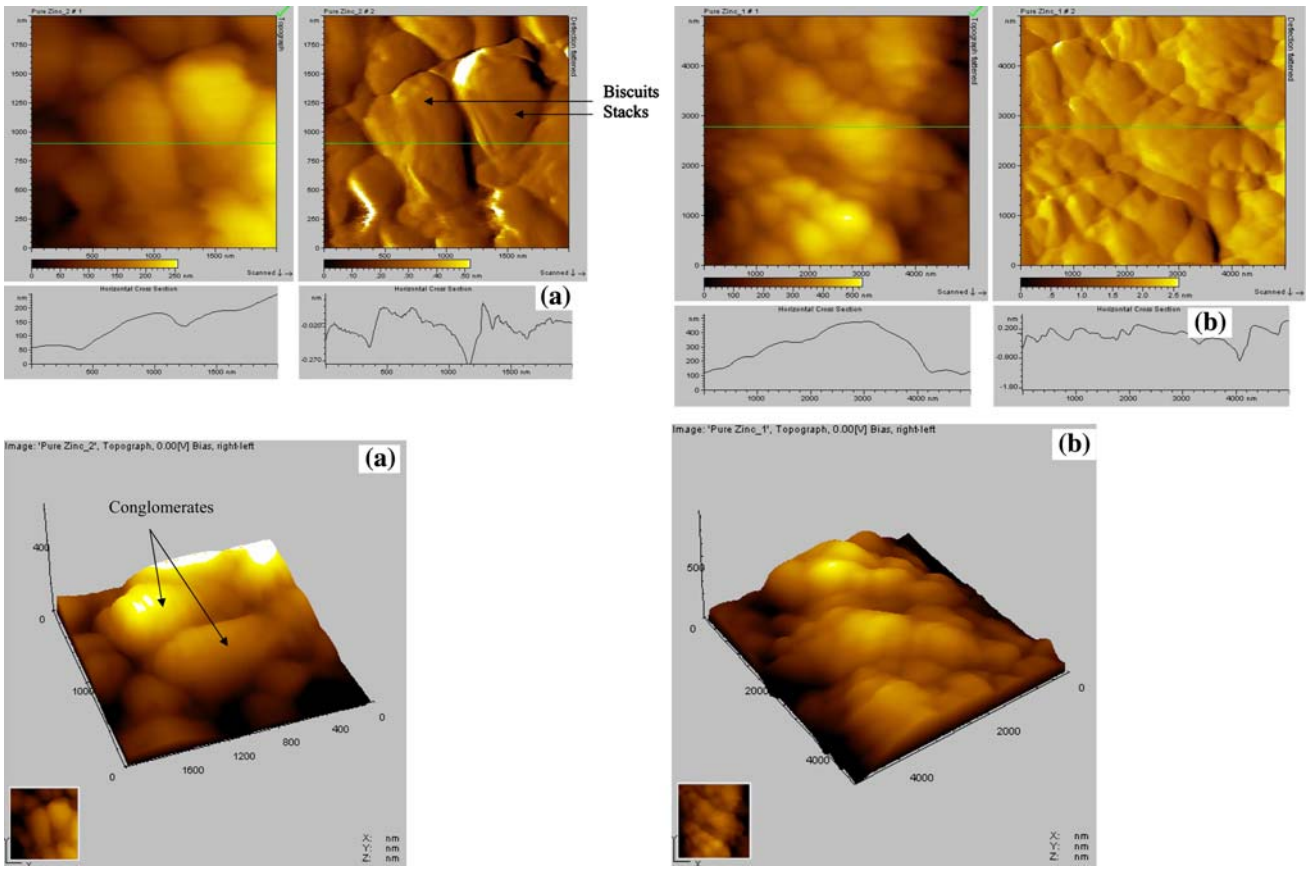

Fig. 2 (**a** & **b**) The AFM image (**a**): surface topography of the zinc coating after 4 h of anodic machining (**b**): surface topography of zinc coating after 8 h of anodic machining

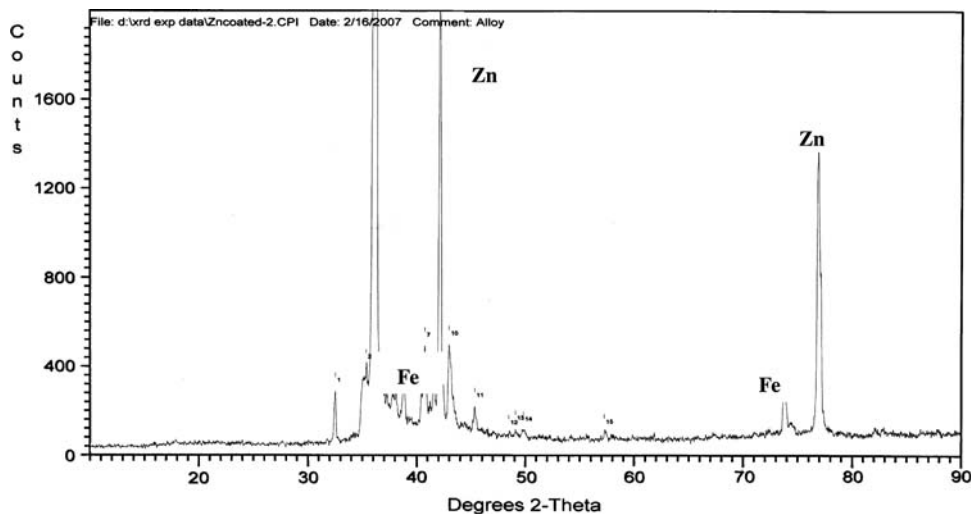

Fig. 3 The XRD analysis of the zinc coating after 4 h of anodic machining

Figure 5 illustrates the variation in potential of the inner alloy layers exposed in saline medium, after electrochemical machining of the galvanized coupons. The potential of the coupons having fresh coating was continuously monitored till a stable equilibrium potential was established. During the initial stage of anodic dissolution, the coupons showed abrupt changes in the OCP values. After each 2-h period of anodic dissolution machining, the characteristic potential of the newly exposed surfaces was measured. The sacrificial nature of zinc on steel was shown by high negative corrosion potential values. The presence of the pure zinc outer layer was associated with a more active

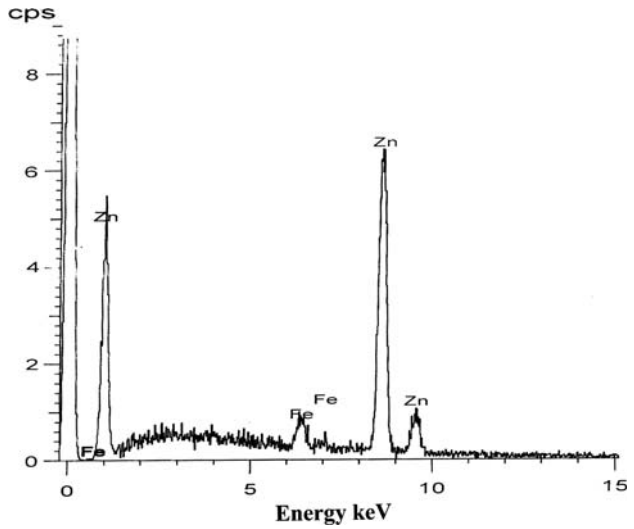

Fig. 4 EDX spectrum of the coating showing presence of Fe and Zn in the alloy layers opened during successive anodic machining steps

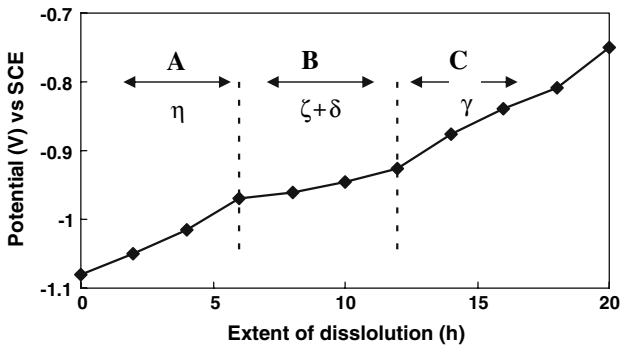

Fig. 5 The variation in potential of the galvanic coating against the extent of dissolution during anodic machining. Electrolyte medium—Stagnant 3% NaCl solution, Current strength—10 mA/cm^2, Temperature—30 ± 2 °C

(negative) potential during anodic machining (η-phase, region 'A' in Fig. 3). However, the outermost layer (pure zinc) dissolved easily without forming a protective layer, resulting in the exposure of inner alloy layers.

As the dissolution progressed exposing successive layers, the inner alloy layers, which contained more iron, exhibited minimum potential shift. At the region 'B', which was supposed to be ζ- & δ-phase, corresponding to that where the concentration of iron was greater and that of zinc was optimum, a slow and steady potential shift was noticed. The ζ-phase consists of monoclinic crystal structure having 5–6 wt% of iron and the balance zinc, and the δ-phase consists of hexagonal structure with 7–12% iron content. The mixed potential established by the Fe–Zn alloy (with its Zn-rich and Fe-rich regions) was sufficient to prevent the drastic potential shift. This behavior of the inner Fe-rich alloy layers was found to be in accordance with the available literature [20–24]. After 12 h of dissolution/electrochemical machining, the OCP shifted to a more anodic region corresponding to the γ-phase, region 'C' in Fig. 5, revealing the probable γ-phase consisting of fcc structure.

Four distinct Fe–Zn phases had formed in layers on the steel substrate, each of which had a different corrosion potential. The top layer (η-phase) consisted of pure zinc (Zn ~ 99.9%) that exhibited a more negative potential; this layer was readily sacrificed to protect layers below. The inner layers of the hot-dip galvanized coating have been reported to contain three different phases, viz: ζ-phase (~94% Zn–6% Fe), δ-phase (87–94% Zn–6–13% Fe) and γ-phase (72–79% Zn–~21–28% Fe) [25]. Among the three phases, the ζ- and δ-phases exhibited more corrosion resistance as was evidenced from the potential changes observed during anodic machining. The steady corrosion potential of these two layers could be attributed to the peculiar surface structure and the type of close packing of the alloy layers. The ζ-phase has a monoclinic structure and contains 94.6% zinc. The δ-phase has a hexagonal structure with a nominal composition of $FeZn_7$ with 89.2% Zn, and $FeZn_{10}$ with 92.1% Zn.

The innermost layer, i.e. the γ-phase, is face centered cubic and is Fe-rich. The zinc in this layer is insufficient to nullify the potential shift during anodic machining. Hence the concentration of iron in the newly exposed inner layers steadily increased during anodic dissolution resulting in a potential sweep of the coating after 12 h. There should be a minimum amount of zinc in the coating to control and maintain a steady potential. The region corresponding to 6–12 h of dissolution (i.e. 'B' [ζ- & δ-phase] in Fig. 5) corresponds to the optimum amount of zinc in the iron–zinc phase that generated a mixed potential with minimum potential shift. This led to effective galvanic protection of the steel.

The layer-wise concentration of both zinc and iron in the coating was estimated after each successive anodic dissolution step and correlated with the potential measured for each layer (Figs. 5 and 6). The electrolyte solution was replaced after each hour interval of electrochemical machining in order to minimize any segregation of the dissolution products that might affect the machining process. The coating composition was determined under the standard conditions by controlled removal of the metal by electrochemical machining.

The concentration profile of Fe and Zn from the outermost layer of the coating toward interior layers of the coating is shown in Fig. 6. There was no variation above 10% in the results. A steady and gradual increase in the Fe content toward the interior layers was observed. The Zn concentration in the electrolyte after machining for 8–12 h showed a little decrease. This depth within the coating, i.e. region 'B' in Fig. 6, had the optimum composition that was

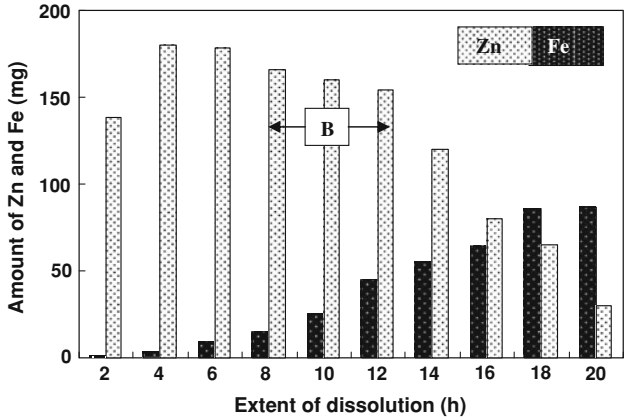

Fig. 6 The profile of zinc and iron concentration in the electrolyte after each anodic machining step. Electrolyte medium—Stagnant 3% NaCl solution, Temperature—30 ± 2 °C

sufficient for exerting galvanic activity. A steady decrease in Zn concentration caused a steady potential shift of the coating toward anodic region. Based on this observation, an independent layer-wise analysis of the galvanic coating was performed.

Layer-wise galvanic performance

The galvanized coupons were machined so that each coupon had a different layer of the coating exposed. These machined coupons were then subjected to anodic polarization up to an applied current density of 100 mA/cm^2. After each 2-h interval of anodic machining, the corresponding coupons were removed and rinsed. The behavior of the inner layers during polarization analysis is shown in Fig. 7. The inner layers were more susceptible to severe polarization than the outer layers. The pure zinc in the outer layers dissolved steadily causing slow polarization. The polarization was high when the anodic machining was proceeded further toward the interior layers due to (a)

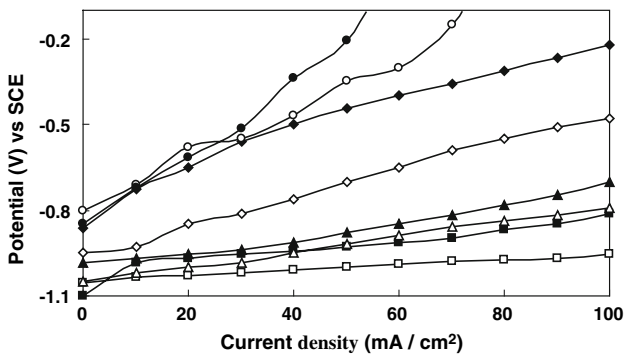

Fig. 7 The polarization trend of the zinc coating after different extent of anodic machining. Electrolyte medium—Stagnant 3% NaCl solution, Temperature—30 ± 2 °C. [□-0 h, ■-2 h, △-4 h, ▲-6 h, ◇-8 h, ◆-10 h, ○-12 h, ●-14 h]

Table 1 The impedance data of the coating subjected to different extent of anodic machining. Medium—3% NaCl solution, Temperature—30 ± 2°

S. No.	The extent of dissolution of the coating (h)	R_s (Ω)	R_p (Ω)	CPE
1	Two	0.6179	38.47	1.42×10^{-2}
2	Six	0.7687	84.74	1.28×10^{-8}
3	Ten	0.7634	83.74	1.33×10^{-8}

compositional change (b) increase in Fe content, and (c) decrease in Zn content. Also a distinct polarization trend, i.e. no fluctuation or abruptness in the polarization trend, was observed after the successive polarization up to 12 h. The deeper layers corresponding to more than 12 h of anodic dissolution exhibited abrupt changes in the polarization trend.

In addition to layer-wise analysis, AC impedance characteristics of these machined layers were also analyzed and interpreted. The AC impedance values of the coatings, after different extents of anodic machining, also exhibited the same trend. Table 1 shows the impedance parameters of the coating. The high R_p values of the coating layers exposed after six and 10 h of machining revealed high corrosion resistance of the corresponding layers compared to the outer pure Zn layer. There were no significant changes in either the value of solution resistance or in the qualitative composition of these inner layers. These observations supported the interpretation that the outer layers, and not the outermost or interior layers, had a significant role on the galvanic activity.

Threshold zinc and the galvanic performance

It is obvious that the difference in the corrosion potentials of the individual layers will affect the overall behavior of the coating. Various mechanisms have been proposed for describing the reaction of iron and zinc [26–32]. However, there are few studies concerning the influence of the various alloy phases on the overall corrosion behavior of the coating under different weathering conditions. The quantity of zinc necessary to give optimum sacrificial protection to the coating under exposed condition was also determined.

Three coupons were subjected to three different extents of anodic machining. The remaining zinc contents in the coating of those coupons were found to be A: 0.0526 mg/cm^2, B: 0.064 mg/cm^2, C: 0.086 mg/cm^2, as estimated with respect to similar machined coupons. The coupons were cleaned with water and immersed in 3% sodium chloride solution. The coupons after anodic machining were exposed to sodium chloride for a period of 60 days. In all these cases there was a potential shift during initial days of exposure (Fig. 8). Zinc

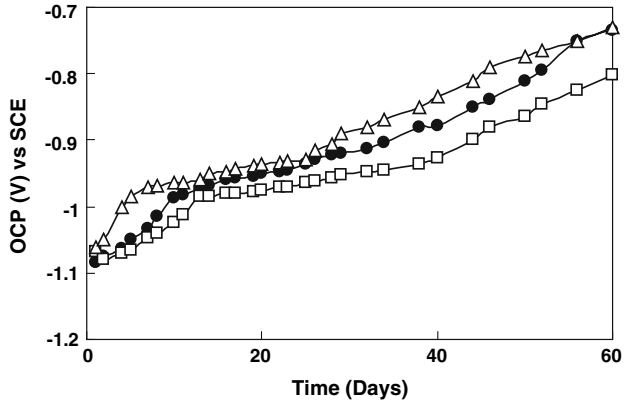

Fig. 8 The variation in potential of different coatings after subjected to different extent of anodic dissolution. The remaining zinc content of the coating after anodic machining, Δ-0.0526 mg/cm^2, ●-0.064 mg/cm^2, □-0.086 mg/cm^2

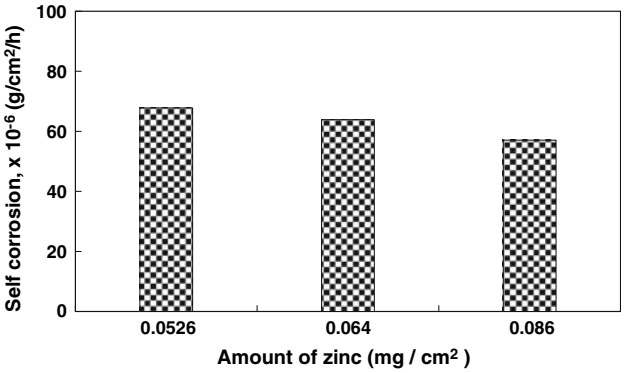

Fig. 9 The self-corrosion rate of the anodically machined zinc coating, after 60 days of immersion, Electrolyte medium: Stagnant 3% NaCl solution. The zinc content of the coating (A) 0.0526 mg/cm^2, (B) 0.064 mg/cm^2, (C) 0.086 mg/cm^2

content still remained in the coating after machining. It was predicted that impermeable oxide layers could not be formed, as there was no sufficient ageing time to grow as a barrier. Hence very low potential shift could be predicted due to insignificant variation in the surface composition. With continued anodic machining of the coating, the shift in potential corresponding to the inner layers was found to be low. In the case of inner alloy layers the presence of iron in the alloy phases lower the potential shift during anodic dissolution. This can be ascribed to the mixed potential offered to the alloy layers due to the presence of iron and zinc in the inner layers as reported elsewhere [20–23].

The coupons exhibited a steady potential shift corresponding to the period of 10–30 days. The potential shifted quickly attained a quasi-steady state in the potential range of −0.975 to −0.950V. The mixed potential of the iron-rich layers and comparatively less voluminous corrosion product prevented drastic shift in the potential values. This was the region where the presence of zinc was just sufficient to minimize the potential shift and this could be assumed to be the threshold zinc level. The slower dissolution of the inner alloy layers could also be attributed to better zinc diffusion into the steel substrate during hot dipping, forming a compact inner Fe–Zn alloy layer which would have more corrosion resistance. After 40 days of exposure, the potential shifted to the more passive region (more anodic). The drastic potential shift beyond that region could be attributed to the substantial changes in the zinc and iron concentration in the coating. The γ-layer having the lowest amount of zinc became exposed and the base steel was attacked. Although there was zinc present in that layer, it was insufficient to cathodically control pit formation leading to localized substrate corrosion. It appeared that the γ-layer provided some cathodic protection around these localized corrosion deposits, inhibiting their growth. It could be inferred that there should be a certain level of zinc content present in the coating so as to protect the steel from corrosion by means of cathodic protection under exposed conditions.

The self-corrosion rates of the as-anodically machined coatings when subjected to long-time immersion are compared in Fig. 9. The corrosion rate was found to be independent of the amount of zinc present in the coating. All the coatings were found to have almost equal self-corrosion values. Hence, we could infer that the efficiency of the coating was not dependent absolutely on the amount of the zinc but also on the morphology and nature of the inner alloy layers including the structural character. This observation was treated as one of the supportive evidence of the above-discussed concept.

Conclusions

The electrochemical characteristics of inner alloy layers of hot-dip coatings were studied by applying the technique of electrochemical machining. It was observed that the outer layers, and not the outermost or the interior layers, had a significant role in the galvanic activity. Among the four phases, the zeta and delta phases showed more corrosion resistance as was evidenced based on the potential changes observed during anodic machining. The impedance values of these phases also revealed effective corrosion resistance of these phases than the pure zinc top layer. The polarization characteristics of the iron-rich inner layers were found to be superior to that of the pure zinc outer layer. The galvanic performance of the inner alloy layers was found to be superior to that of the outer layers. The total zinc content in the coating was not the absolute parameter of the protection capacity of the coating. The corrosion resistance performance of the coating not only depended on the outer

layer zinc content but also significantly on the inner alloy zinc concentration.

Acknowledgement We thank Prof. Dr. P. Indrasenan, Head, Dept. of Chemistry, University of Kerala, for his kind administrative help.

References

1. Horng YT, Lin JH, Hsu JW, Shih HC, Wang JH, Chang TC, Hsu HP, Lin YC (2003) Mater Perform 42:32
2. Vosgien JM (2002) Revue de Metallurgie/Cahiers d' Information Techniques, (Fr), vol 99, p 709
3. Reumont G, Vogt JB, Iost A, Foct J (2001) Surf Coat Technol 139:265
4. Bablik H (1950) Hot-dip galvanizing. E.F.N. Spon Ltd, London
5. Ferrier A (1979) Mem Et Sci Rev Met 76:777
6. Kubaschewaski O (1982) Iron binary phase diagram. Springer-Verlag, Berlin, p 172
7. Dauphin JY, Perrot P, Tchissambot UG (1987) Mem Et Sci Rev Met 84:329
8. Massalski TB (1990) Binary alloys phase diagrams, 2nd edn. ASM Hand book, p 1795
9. Kubota H, Kusakabe T, Hata S (2001) Japanese Patent 247 947
10. Carlsson P, Bexell U, Olsson M (2001) Wear 247:88
11. Blau PJ (1992) Friction, lubrication and wear technology, glossary of terms, vol 18. ASM Handbook
12. Rigney DA, Chen LH, Naylor MGS, Rosenfield AR (1984) Wear 100:195
13. Lohrengel MM, Rosenkranz Chr (2004) Corros Sci 47:785
14. Ebeid SJ, Hewidy MS, El-Taweel TA, Youssef AH (2004) J Mater Process Tech 149:432
15. Haisch T, Mittemeijer E, Schultze JW (2001) Electrochim Acta 47:235
16. Datta M, Landolt D (1980) Electrochim Acta 25:1255
17. Biber HE (1988) Metall Trans A 19:1603
18. Strutzenberger J, Faderl J (1998) Metall Mater Trans A 29:631
19. Vincent G, Bonasso N, Lecomte JS, Colinet B, Gay B, Esling C (2006) J Mater Sci 41:5966
20. Vazquez AJ, De damborenea JJ (1992) Brit Corros J 27:310
21. Frappe AL, Linare A, Piessen P, Vacher JC (1985) Proceedings of the 14th international conference on hot-dip galvanizing, intergalva (EGGA)'85, London, pp 8.1–8.18
22. Johnsson T, Kucera V (1982) Proceedings of the 13th international conference on hot-dip galvanizing, intergalva (EGGA)'82, London, pp 47.1–47.6
23. Westerlund R (1979) Proceedings of the 12th international conference on hot-dip galvanizing, intergalva (EGGA)'79, London, p 320
24. Reumont G, Perrot P, Foct J (1998) J Mater Sci 33:4759
25. Burns RM, Bradley WW (1967) Protective coatings for metals, 3rd edn. Reinhold Publishing Corporation
26. Giorgi ML, Guillot JB, Nicolle R (2005) J Mater Sci 40:2263
27. Chirazi A, Quintin AP, Reumont G, Foct J (2007) Iron Steel Technol 4:193
28. Fenoel MNA, Reumont G, Goodwin F, Perrot P, Foct J (2006) Int J Mat Res 97:1183
29. Quintin AP, Fenoel MNA, Chirazi A, Reumont G, Foct J, Goodwin F (2005) AISTech 2004—Iron and steel technology conference proceedings, vol 2, p 511
30. Reumont G, Perrot P, Dupin N, Dutheillet Y (2003) J Mater Sci Lett 22:975
31. Reumont G, Maniez S, Gay B, Perrot P (2000) J Mater Sci Lett 19:2081
32. Reumont G, Figeuiredo RSD, Foct J (1999) J Mater Sci Lett 18:1879